Simultaneous Size, Layout, and Topology Optimization of Stiffened Panels using CAD-based Parameterization

Rahman, H.; De Breuker, R.; Castro, Saullo G.P.

DOI
10.2514/6.2023-1090

Publication date
2023

Document Version
Final published version

Published in
AIAA SciTech Forum 2023

AIAA SciTech Forum
23-27 January 2023, National Harbor, MD & Online
AIAA SCITECH 2023 Forum

10.2514/6.2023-1090

Simultaneous Size, Layout, and Topology Optimization of Stiffened Panels using CAD-based Parameterization

Hammad Rahman[1], Roeland De Breuker[2] and Saullo G. P. Castro[3]
Delft University of Technology, Delft, 2629 HS, The Netherlands

In this paper, an innovative design methodology is proposed to simultaneously optimize the size, layout, and number of stiffeners of a stiffened panel using a gradient-based optimizer. In the proposed method, CAD-based parameterization is used to parameterize the layout of the stiffeners. The location and orientation of each stiffener are controlled with only two layout variables. The geometric constraints to avoid overlapping and crossing of stiffeners are implicitly applied through the layout parameterization scheme, therefore no additional constraints on the grid point coordinates are required. Moreover, the CAD model is maintained throughout the optimization process therefore the additional step of converting the optimal design back to CAD is eliminated. The layout changes are accommodated in the finite element mesh through the re-meshing technique. The number of stiffeners is controlled by allowing an optimizer to transform an existing stiffener into a ghost stiffener. Every stiffener is assigned a topology variable that can be optimized to a value of either 0 or 1 using a penalization constraint. In case the optimal value is 0 then the contribution of that stiffener in determining the mass and the stiffness of the panel is lost and it is considered an inactive or ghost stiffener. The stiffener is considered fully active when the optimal value is 1. The sensitivities of grid point coordinates relative to layout variables are calculated analytically. The sensitivities of the structural responses relative to size, layout, and topology variables are achieved through Nastran. The effectiveness of the proposed methodology is evident from the obtained results.

I. Nomenclature

CAD	=	computer-aided design
BLF	=	buckling load factor
FFD	=	free-form deformation
p	=	penalization factor

II. Introduction

Stiffened panels are extensively used in aerospace and marine applications because of their high specific stiffness and strength. In aircraft, they are used to build the structure of wings and fuselage. The structure of a stiffened panel is constructed by joining a thin skin panel with stiffeners as shown in Fig. 1. The stiffeners are attached for the reinforcement of the skin. Since a stiffened panel is a thin-walled structure, therefore besides strength failure, it is prone to fail under buckling instability. The stiffness of the panel can be tailored to achieve the required buckling load factor (BLF). Considering the requirements related to performance, economy, and safety, optimization methods are generally employed to minimize the mass of the stiffened panel while tailoring its stiffness to achieve the desired design response. One such method is topology optimization which is used to determine the optimal material distribution within the design space [1], [2]. It is best suited for design problems where the initial configuration is not

[1] PhD Student, Aerospace Structures and Materials, Email: h.rahman@tudelft.nl
[2] Associate Professor, Aerospace Structures and Materials, AIAA Associate member.
[3] Assistant Professor, Aerospace Structures and Materials.

known therefore a design domain discretized with 3D elements is generally used as the initial design. During the optimization, the best possible combination of shape and size for the desired objective is achieved by removing the elements which do not contribute to the stiffening of the structure. In this way, the greatest design freedom is ensured but at a very high computational cost. In Ref. 1, topology optimization of a wing was performed using 1.1 billion solid elements. It took 5 days of computing time on 8000 CPUs even though only the stiffness was considered for optimization under three linear static loads. Since buckling analysis is time intensive, therefore for the design problems involving thin-walled structures, the efficient approach used in literature, is to discretize the design domain with 2D shell elements and parameterize it with the size, layout, and topology variables. The size variables control the thicknesses of the skin and stiffeners, layout variables control the placement of the stiffeners on the skin including their location and orientation, and topology variables control the number of stiffeners. Traditionally, a stiffened panel is designed using size optimization while keeping the layout and the topology variables fixed. If the layout configuration and the number of stiffeners are predetermined then a limited mass saving can be achieved. For additional mass saving, it is important to perform simultaneous optimization of size, layout, and topology variables. Therefore, various studies on this area of research were conducted in the last decade [3]–[7]. In these studies, a gradient-free optimizer was used which usually requires a higher number of evaluations when compared to a gradient-based optimizer. The gradient-free optimizers are more applicable to models that require a small computational cost or involve a limited number of design variables. These limitations limit the possible improvement in the structural performance that can be achieved through optimization. Therefore, in some recent studies, a gradient-based optimizer was employed [8]–[10]. The internal topology of each stiffener was optimized which allowed the optimizer to partially remove the stiffener. This resulted in the optimal designs that can be difficult to manufacture. A mesh morphing strategy based on the Free-Form Deformation (FFD) method was used to manipulate the finite element mesh to accommodate the perturbed layouts generated during the optimization. The use of mesh morphing requires additional constraints on the grid point coordinates to ensure that the adjacent stiffeners do not overlap or cross each other in the deformed meshes. The sensitivities of such constraints were computed using the finite difference method, which also significantly increased the computational cost. Moreover, FFD does not allow large changes in the layout because of mesh distortion issues. It also poses a limitation while working directly with the computer-aided design (CAD) models of the configurations.

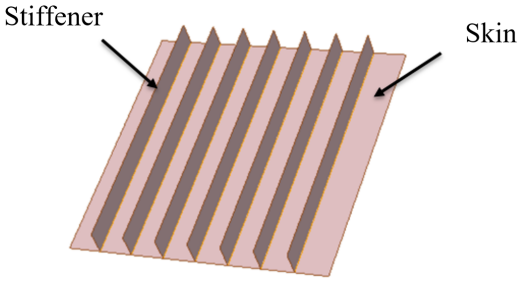

Fig. 1: Stiffened panel structure

The research herein presented tries to overcome these limitations by developing an innovative design methodology that employs a CAD-like modeling tool to parameterize the stiffened panel geometry, generate the finite element mesh and provide the geometric sensitivities which are the derivatives of the grid point coordinates relative to the layout design variables. The use of this CAD-based parameterization offers two advantages. Firstly, the geometric constraints to avoid overlapping and crossing of stiffeners are implicitly applied through the layout parameterization scheme, therefore no additional constraints on the grid points coordinates are required. Secondly, the CAD model is maintained throughout the optimization process because the CAD variables are directly controlled by the optimizer. Therefore, the additional step of converting the optimal design back to CAD is not required. The internal topology of each stiffener is fixed therefore either the whole stiffener will stay or disappear from the panel. This is achieved by allowing the optimizer to transform a stiffener into a ghost stiffener. The ghost stiffeners do not contribute to the mass and stiffness calculations of the panel. A re-meshing strategy is used instead of FFD to allow large changes in the layout. The developed tool chain employed commercially available tools. This is crucial for the wider adoption of the proposed methodology in the industry.

The remainder of this paper is organized as follows. The design methodology is introduced in Section 3. The design problem is formulated and explained in Section 4. The results of the stiffened panel design are presented and discussed in Section 5. The conclusions are given in section 6.

III. Design Methodology

The stiffened panel geometry was modeled in Engineering Sketch Pad (ESP) [11]. ESP is a CAD-like feature-based solid modeling tool built on OpenCSM, OpenCASCADE geometry kernel, and EGADS geometry generation system. It can model a common CAD configuration for different analysis disciplines of varying fidelities [12]. The layout parameterization was defined in ESP. The geometric constraints to avoid overlapping and crossing of stiffeners were implicitly applied through the layout parameterization, which eliminated the requirement of applying additional constraints on the grid points coordinates. The surface-based mesh was created in ESP. To accommodate the perturbed layouts, a re-meshing strategy was used instead of mesh morphing to avoid the mesh distortion issue. For defining the CAD parameters of ESP as layout design variables in the optimization, geometric sensitivities are required. The geometric sensitives are the derivatives that define the change in the position of a point lying on the CAD model boundary relative to a unit change in the layout variable. ESP can calculate these derivatives analytically [13], [14]. These derivatives were included in the Nastran design sensitivity analysis using the DVGRID cards. The response sensitivities relative to the design variables were achieved from the Nastran design sensitivity analysis. Nastran uses a semi-analytical method to calculate these sensitivities and it is more computationally efficient than the finite element methods [15]. In the topology optimization literature, solid isotropic material with penalization (SIMP) method [16], [17] is extensively used. In this method, an artificial material and a topology design variable are assigned to each element. The topology variable can vary between 0 and 1. Its relationship with artificial material properties is expressed as follows:

$$\rho = \rho' * (x_T)$$

$$E = E' * (x_T)^p$$

where, ρ and E are the density and Young's modulus of the artificial material, respectively; ρ' and E' are the density and Young's modulus of the base material, respectively; x_T is the topology variable; p is a penalization factor. The role of the penalization factor is to force the topology design variable to be close to either 0 or 1, therefore the value of p is always greater than 1. The decision on retaining or removing an element is based on the value of x_T. If the value of x_T is 0 then that element is removed from the design space. A similar concept is used in this study with a modification to limit the computational cost. All the elements of a single stiffener are assigned the same topology variable. Therefore the number of required topology design variables is equal to the number of stiffeners. During the optimization, if the topology design variable of a stiffener becomes 0, then the contribution of that stiffener in determining the mass and the stiffness of the panel will be lost. It will be considered an inactive or ghost stiffener. The term ghost stiffener is used because the elements of the stiffener will be present throughout the optimization process but their contribution regarding mass and stiffness will be lost. It is pertinent to mention that the size and layout variables of the stiffener are optimized even when it becomes a ghost stiffener. In this work, the topology optimization problem was set up in Nastran. The artificial material was defined using the DVMREL2 and the DEQATN cards. It was observed that despite the use of p, it was difficult for the optimizer to push all the topology design variables to their limit values, therefore an additional penalization constraint was applied to each topology design variable. The penalization constraint was defined as follows:

$$(x_T - {x_T}^2) \leq 0.0001$$

A similar penalization constraint was used to find the optimal control surface layout of an aircraft in Ref. 16. In the proposed method, the penalization constraints were defined in Nastran using the DEQATN cards. The response sensitivities relative to topology design variables were calculated in Nastran using the design sensitivity analysis. At the end of optimization, the ghost stiffeners can be removed from the CAD model. The optimization problem was set up in OpenMDAO [18] and a gradient-based optimizer, SLSQP was used to find the optimal design. The flow chart of the proposed method is shown in Fig. 2. In every design iteration, a parameterized CAD model was created in ESP. The geometric sensitivities relative to every layout design variable were calculated and using this data the DVGRID cards were printed for every layout design variable and grid point pair. These cards were included in the Nastran input file for SOL200. The input data for mesh, boundary conditions, loads, objective function, constraints, and design variables were stored in the same file. The design sensitivity analysis was conducted in Nastran. The objective, constraints, and their gradients were transferred to the external optimizer. These steps were repeated in every design iteration till convergence.

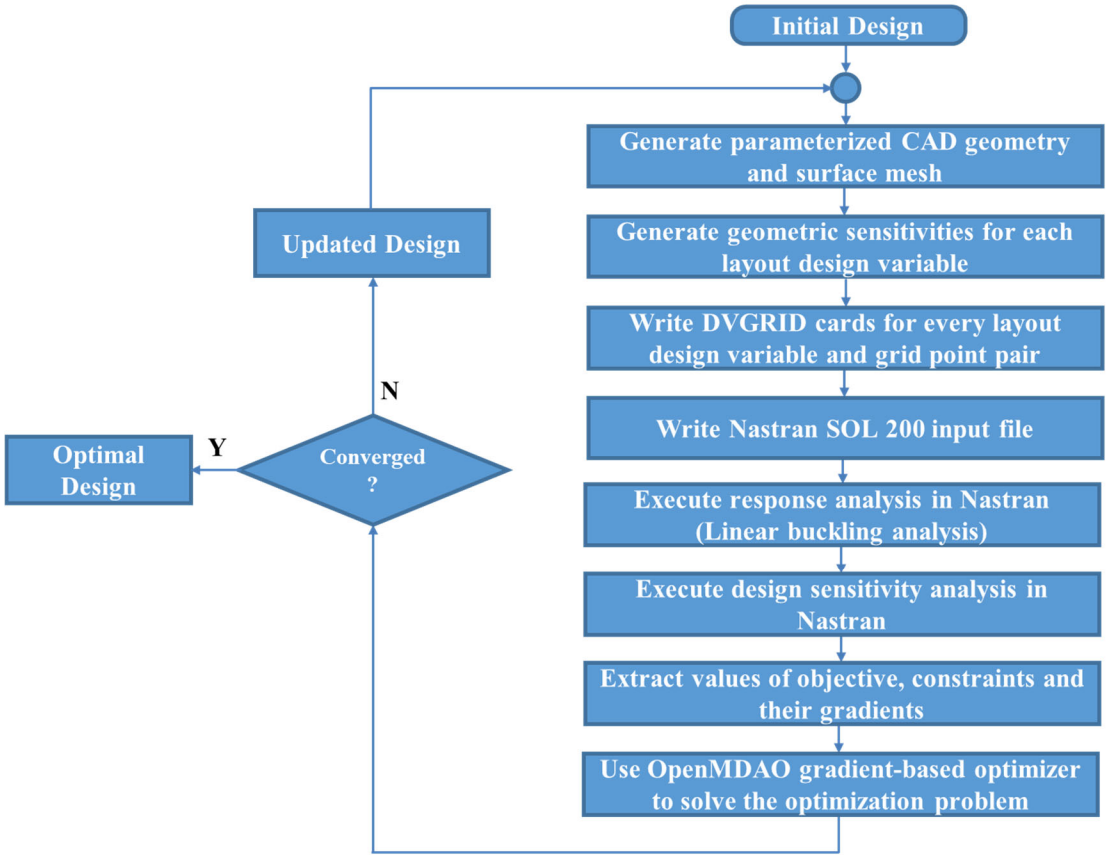

Fig. 2: Flow chart of the proposed method

IV. Design Problem Formulation

A. Stiffened Panel Geometry

The stiffened panel geometry of Ref. 8 was used in the work presented in this paper. The geometry was modeled in ESP. The surface mesh was generated using ESP and egadsTessAIM [19]. The CAD model, finite element mesh, and the applied boundary conditions are shown in Fig. 3. The panel included 7 blade stiffeners each with a fixed height of 0.03m. A shear load of 300 KN/m was applied at the top edge of the skin. The skin and each stiffener were discretized with 80 x 80 and 8 x 80 CQUAD4 shell elements, respectively. The isotropic material properties used in Ref. 8 are Young's modulus = 73GPa, Poisson's ratio = 0.33, and density = 2795kg/m^3.

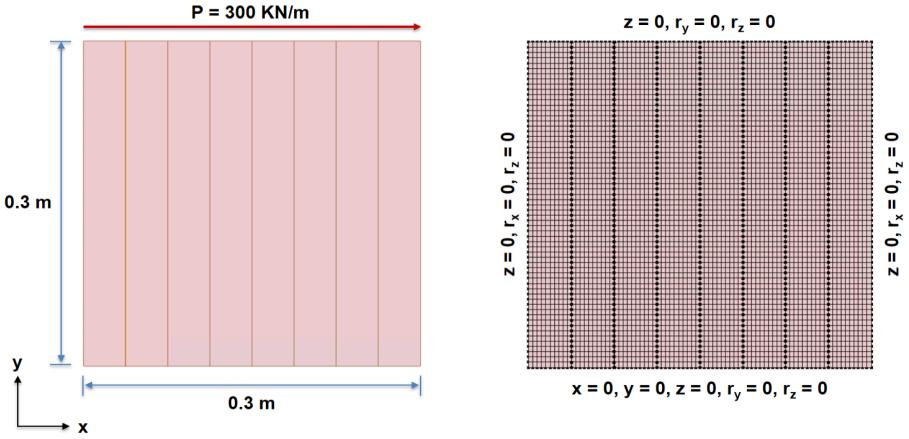

Fig. 3: Stiffened panel CAD model and finite element mesh

B. Size parameterization

The size design space was parameterized using 8 design variables, represented by $x_{S,i}$ (where, i = 1,2,…,8). This parameterization included one design variable defining the thickness of the skin and 7 design variables defining the thicknesses of 7 stiffeners.

C. Layout parameterization

The layout of the stiffened panel was parameterized using a CAD-based parameterization. The CAD model in ESP was generated in such a way that the location and the orientation of each stiffener were controlled with only two design parameters. The illustrations of the layout parameterization scheme for the first and second stiffeners from the left side of the panel are shown in Fig. 4(a) and 4(b), respectively. The panel skin is represented by the square ABCD. It is evident from Fig. 4(a) that point x_1 is located on line AB. The location of this point was defined as the fraction of length L_1. Similarly, point x_2 is located on line CD and was defined as a fraction of length L_2. Stiffener 1 is represented by the line connecting the points x_1 and x_2. Since the placement of this stiffener can be controlled through points x_1 and x_2, therefore the locations of these points were defined as layout design variables for stiffener 1. The stiffener can be positioned between its lower and upper limits shown as blue dotted lines u_1u_2 and v_1v_2, respectively. These limits were defined by the lower bound (L.B) and the upper bound (U.B) values of the layout design variables. After the placement of stiffener 1, L_1 and L_2 were re-adjusted as shown in Fig. 4(b). Stiffener 2 was placed in the region marked by x_1BDx_2. Similarly, stiffener 3 was placed in the region marked by y_1BDy_2. Using this CAD-based parameterization, the issues like overlapping and crossing of stiffeners were avoided. This parameterization scheme was very effective because the location and the orientation of 7 stiffeners were controlled with only 14 design variables, represented by $x_{L,j}$ (where, j = 1,2,…,14). Hence, greater design freedom was achieved through a limited number of design variables.

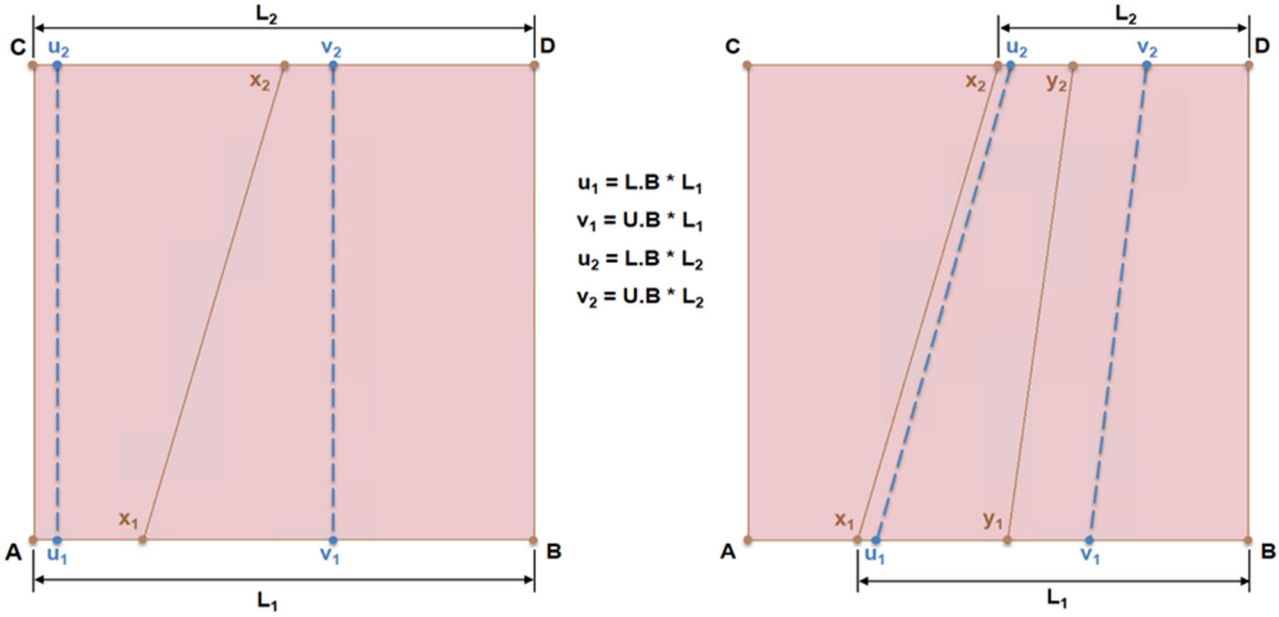

(a) (b)

Fig. 4: Illustration of the layout parameterization scheme: (a) Stiffener 1 parameterization; (b) Stiffener 2 parameterization

D. Topology parameterization

To parameterize the number of stiffeners, 7 design variables, represented by $x_{T,k}$ (where, k = 1,2,…,7), were used to define the topology of 7 stiffeners. The topology variable of a stiffener was used to calculate the material properties (E and ρ) of the artificial material assigned to that particular stiffener. The lower and upper limits for every topology variable were defined as 0.0 and 1.0, respectively. The internal topology of the stiffener was fixed therefore, either the whole stiffener was intact or transformed into a ghost stiffener.

E. Optimization problem

The stiffened panel optimization problem was formulated as follows:

$$\begin{aligned} &minimize && m(x_{S,i}\, x_{L,j}\, x_{T,k}) \\ &subject\ to && \lambda_n(x_{S,i}\, x_{L,j}\, x_{T,k}) \geq 1.0 && n = 1,2,\dots,10 \\ & && (x_{T,k} - {x_{T,k}}^2) \leq 0.0001 && k = 1,2,\dots,7 \end{aligned}$$

The objective was to minimize the mass (m) of the stiffened panel and 10 buckling load factors (λ_n) were constrained to avoid the mode switching. Additional 7 penalization constraints were defined to force the topology variables to have a value of either 0 or 1. A total of 29 design variables were defined, which included 8 size, 14 layout, and 7 topology design variables. Their initial design values and bounds are provided in Table 1.

Table 1: Initial design data

Design Variable Type	Design Variable	Initial Value
Size [L.B = 0.001, U.B = 0.003]	DV 1	0.002
	DV 2	0.002
	DV 3	0.002
	DV 4	0.002
	DV 5	0.002
	DV 6	0.002
	DV 7	0.002
	DV 8	0.002
Layout [L.B = 0.05, U.B = 0.6]	DV 9	0.125
	DV 10	0.125
	DV 11	0.143
	DV 12	0.143
	DV 13	0.167
	DV 14	0.167
	DV 15	0.2
	DV 16	0.2
	DV 17	0.25
	DV 18	0.25
	DV 19	0.333
	DV 20	0.333
	DV 21	0.5
	DV 22	0.5
Topology [L.B = 0.0, U.B = 1.0]	DV 23	1.0
	DV 24	1.0
	DV 25	1.0
	DV 26	1.0
	DV 27	1.0
	DV 28	1.0
	DV 29	1.0

V. Results and Discussion

A. Simultaneous Size and Topology Optimization of the Stiffened Panel

The buckling analysis of the initial design was conducted and the results, including the thickness distribution and the eigenvectors, are displayed in Fig. 5. It is evident from the eigenvectors that the panel underwent buckling at the right bottom side due to the in-plane bending generated by the applied shear load. It is evident from the mode shape results that the global buckling mode is localized between the stiffeners. Using this initial design, size optimization of the stiffened panel was performed and the results are shown in Fig. 6. In modes 1 and 4, the skin of the panel was buckled while in modes 2 and 3, the second stiffener from the left side of the panel was buckled. The trend herein observed is that the thickness of the skin was slightly reduced by the optimizer to meet the buckling constraint. The

thicknesses of all the stiffeners were reduced to their lower bounds because the stiffeners were not directly loaded and the in-plane bending load was transferred to them through the skin. This loading condition was used to benchmark the results against Ref. 8. The mass of the optimized design is 0.675 kg which is 21.1% lower than the initial design mass.

Simultaneous size and topology optimization of the stiffened panel was performed and to hold a comparison with the sizing optimization results, the same initial design was used. The results are presented in Fig. 6. The mass of the optimized design is 0.627 kg which is 26.7% lower than the initial design mass. It can be observed that a greater mass saving is achieved here. The reason for this is the presence of ghost stiffeners in the optimal design. The ghost stiffeners are shown in red in Fig. 8(b). During the optimization, the topology variables of the first and second stiffeners from the left side of the panel were reduced to zero. This removed their contribution to determining the mass and the stiffness of the panel, and hence they became the ghost stiffeners. Another important observation is that modes 2 and 3 of the size optimal design did not appear in the eigenvectors of simultaneous size and topology optimal design. It happened because the stiffener shown buckled in these modes was transformed into a ghost stiffener during the simultaneous size and topology optimization.

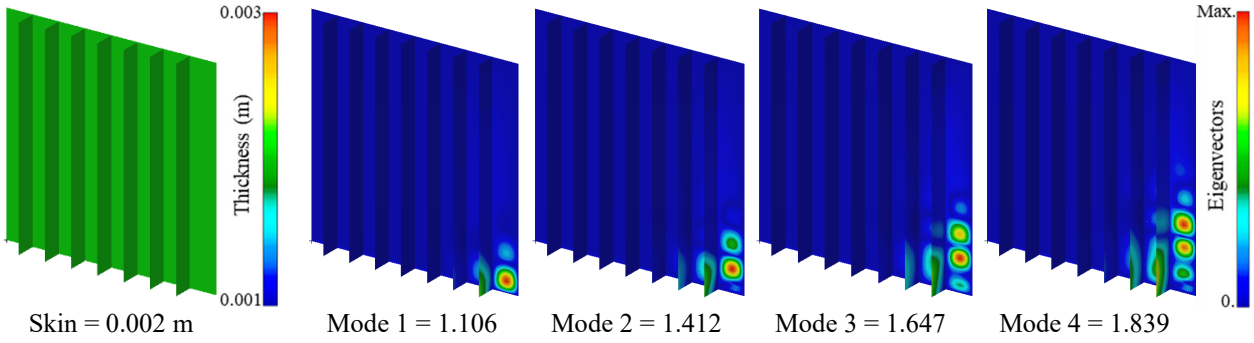

Fig. 5: Initial design of a stiffened panel with 7 stiffeners; m = 0.855 kg

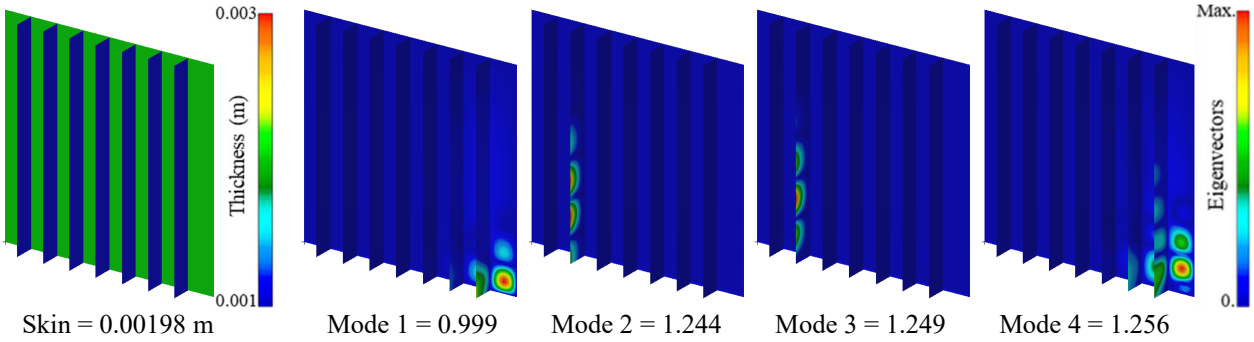

Fig. 6: Size optimal design of a stiffened panel with 7 stiffeners; m = 0.675 kg

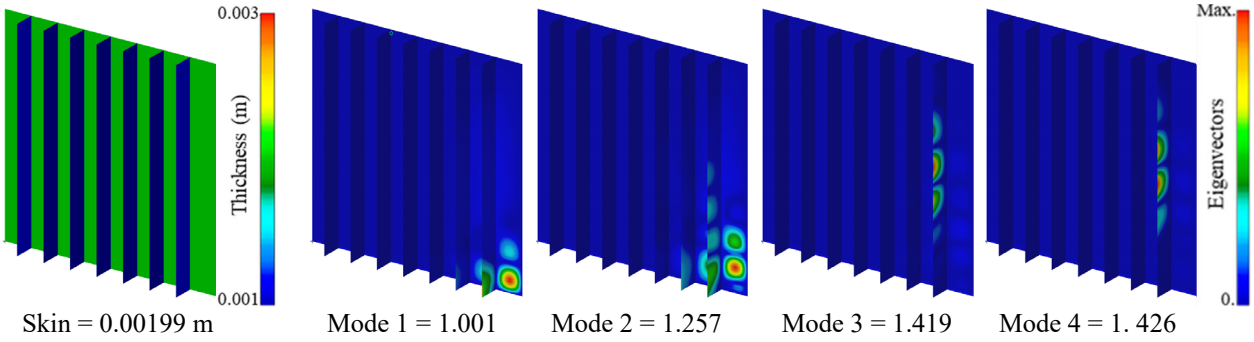

Fig. 7: Simultaneous size and topology optimal design of a stiffened panel with 7 stiffeners; m = 0.627 kg

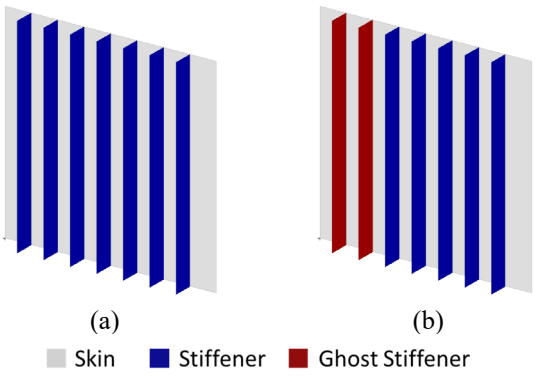

Fig. 8: Optimal stiffened panel CAD models: (a) Size Optimal; (b) Simultaneous size and topology optimal

The convergence of mass and the first BLF during the simultaneous size and topology optimization of the stiffened panel are plotted in Fig. 9. The convergence of the size and the topology design variables are presented in Fig. 10. It is evident from these plots that the size optimization was initially conducted without considering the penalization constraints and only the buckling constraints were included. The optimized design was achieved after 25 design iterations with an optimal mass of 0.613 kg. It can be seen in Fig. 10(b) that the topology design variables associated with the first six stiffeners from the left side of the panel were optimized to some intermediate values between 0.0 and 1.0. As a result, deteriorated material properties of the baseline material were assigned to these stiffeners because the topology design variable of each stiffener was responsible to determine the elastic modulus and the density of the artificial material assigned to that stiffener. To force the values of the topology variables to be either 0.0 or 1.0, the size optimization was restarted from the previous optimal design with the addition of the penalization constraints. The optimum solution was achieved after 16 design iterations. With the help of penalization constraints, the topology variables associated with stiffeners 1 and 2 were pushed to the value of 0.0 because they were previously optimized to a value less than 0.5 during the initial size optimization. The topology variables of the remaining stiffeners were pushed to the value of 1.0 because they were previously optimized to a value greater than 0.5 during the initial size optimization. The final size optimization yielded an optimal mass of 0.627 kg. While comparing it with the optimal mass achieved from the initial size optimization, a small mass penalty was observed which can be attributed to the presence of the penalization constraints in the final size optimization.

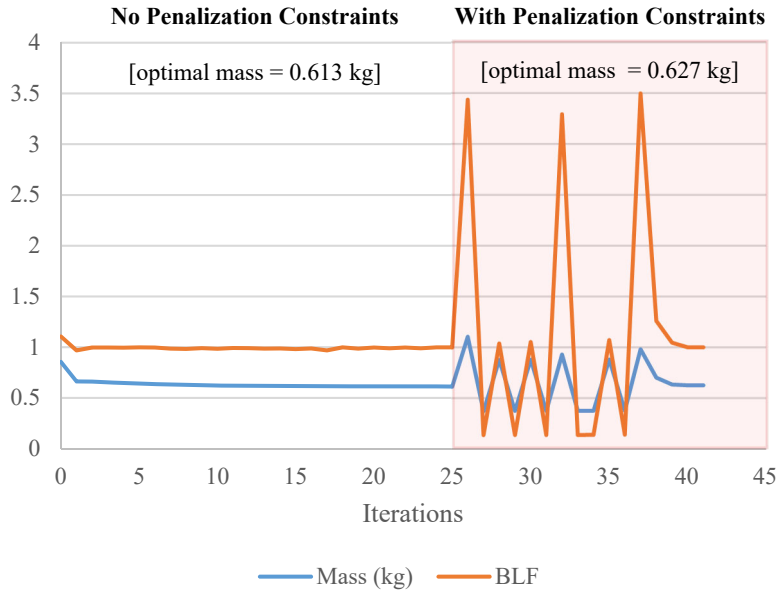

Fig. 9: Convergence curve of the mass and the first BLF

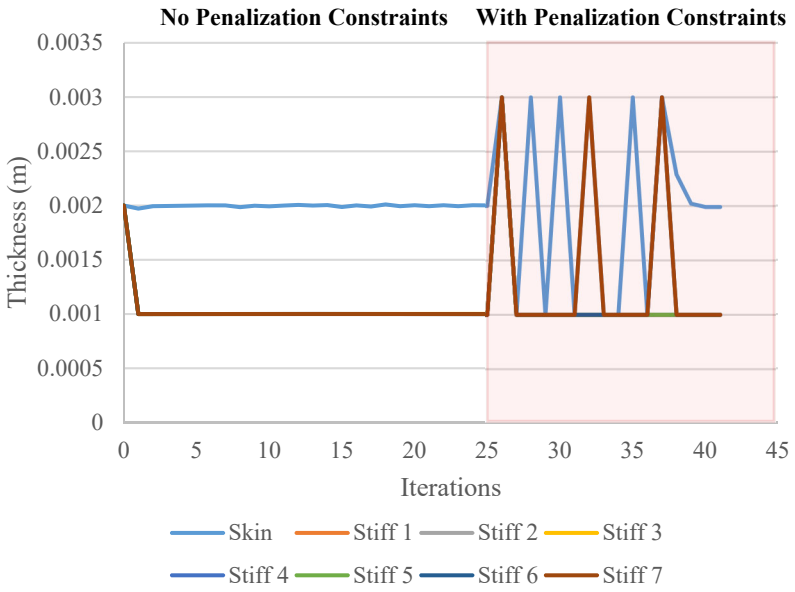

(a)

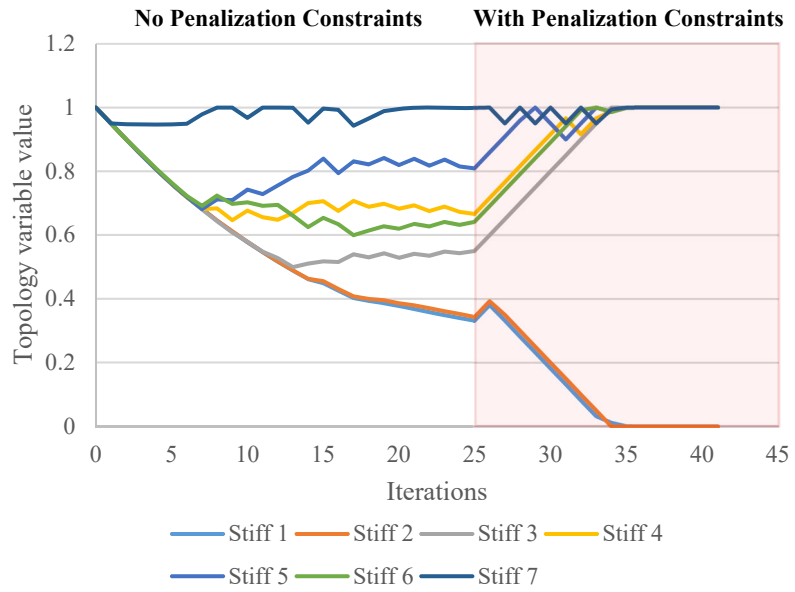

(b)

Fig. 10: Convergence curves of the design variables: (a) Size design variables; (b) Topology design variables

The optimal mass can be sensitive to the initial design used in the simultaneous size and topology optimization. Therefore, additional investigations were conducted using different initial designs generated by changing the initial values of the topology design variables and the parameter p. It is pertinent to mention that all the topology variables of an initial design were assigned the same initial value. The results are shown in Fig. 11, 12, and 13. It can be observed that the optimal mass was marginally affected by the initial values of the topology design variables. The only exception was found at $p = 4$ while using 0.8 as the initial value of the topology design variables. In this case, another local optimum was found by the optimizer which was inferior in comparison to the optimums found while using 0.6 and 1.0 as initial values of the topology design variables. It is also observed that the number of ghost stiffeners in an optimal design was strongly influenced by the value of parameter p. At $p = 2$, the number of ghost stiffeners was

higher than the number of stiffeners. This resulted in the loss of stiffness. To compensate for this loss, the skin thickness was increased by the optimizer, therefore a heavier optimal design was found. The number of ghost stiffeners decreased with the increasing value of p. The best combination of stiffeners and ghost stiffeners which yielded the lowest optimal mass was found at $p = 4.0$ while using 0.6 or 1.0 as initial values for topology design variables. There were no ghost stiffeners at $p = 5$, and the optimum mass was the same as achieved through size optimization.

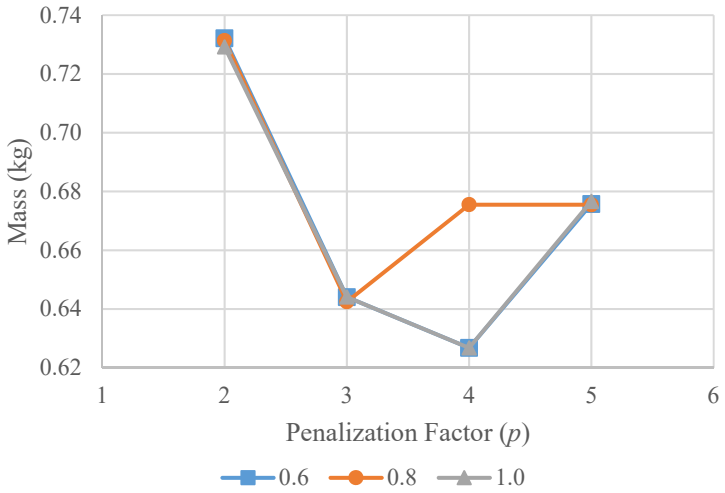

Fig. 11: Effect of different initial values of topology design variables and the parameter p on the optimal mass

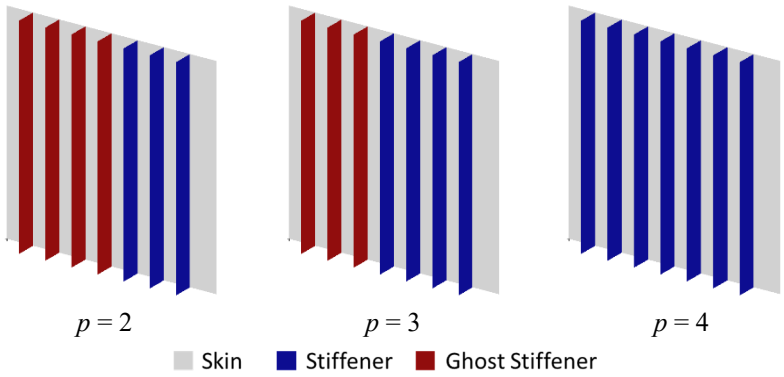

Fig. 12: Optimal stiffened panel CAD models achieved using 0.8 as the initial value of topology variables

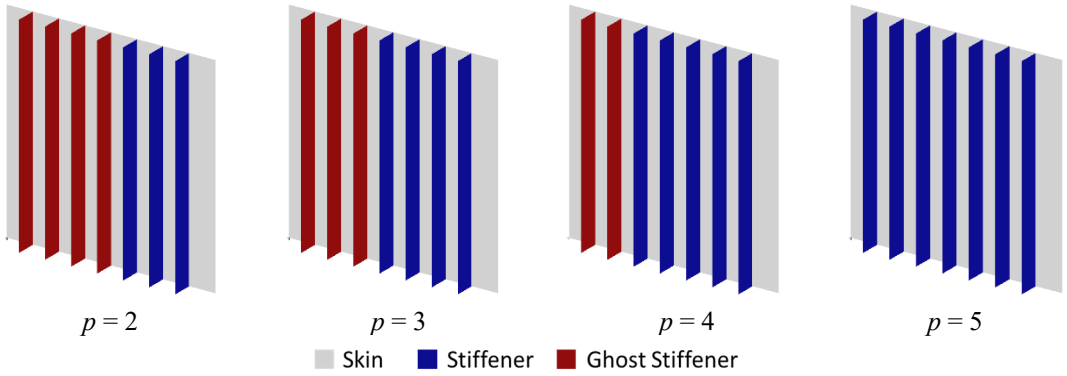

Fig. 13: Optimal stiffened panel CAD models achieved using 1.0 as the initial value of topology variables

The initial designs with different numbers of stiffeners were also investigated. In these studies, the topology variables were assigned an initial value of 1.0. The results are shown in Table 2 and Fig. 14 – 16. The general trend herein observed is that an initial design with more stiffeners can produce a better optimum because the distance between the stiffeners decreases with the increase in the number of stiffeners. This increases the stiffness of the panel. This behavior is further exploited in the simultaneous size and topology optimization. It can be observed that at the right side of the panel, the distance between the stiffener and the edge of the skin is decreased with the increase in the number of stiffeners. Therefore the stiffness in this desired region is increased with the addition of stiffeners. The overall mass is further reduced by transforming additional stiffeners on the left side of the panel into ghost stiffeners. It is evident from Fig. 16 that the initial design with 9 stiffeners and $p = 4.0$ produced the lowest mass. At $p = 2$, the number of ghost stiffeners was higher than the number of stiffeners, therefore a heavier optimal design was found. At $p = 5$, there were no ghost stiffeners, therefore the optimum mass was the same as achieved through the size optimization. It can be concluded from these results that the lowest optimal mass through simultaneous size and topology optimization can be ensured while using 1.0 as the initial value of all the topology design variables and the parameter p in the range from 3.0 – 4.0.

Table 2: Results summary for initial designs with different numbers of stiffeners

Number of Stiffeners	Mass (kg)			Size Optimal Relative Difference (%)	Size + Topology Optimal Relative Difference (%)
	Initial Design	Size Optimal	Size + Topology Optimal		
5 ($p = 3$)	0.755	0.709	0.660	6.09	12.58
7 ($p = 4$)	0.855	0.675	0.627	21.05	26.67
9 ($p = 4$)	0.956	0.667	0.608	30.23	36.40

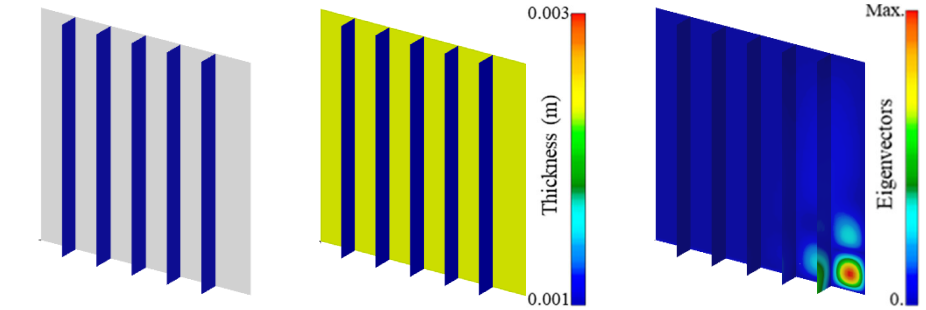

CAD Model, m = 0.709 kg Skin = 0.002320 m Mode 1 = 1.0

(a)

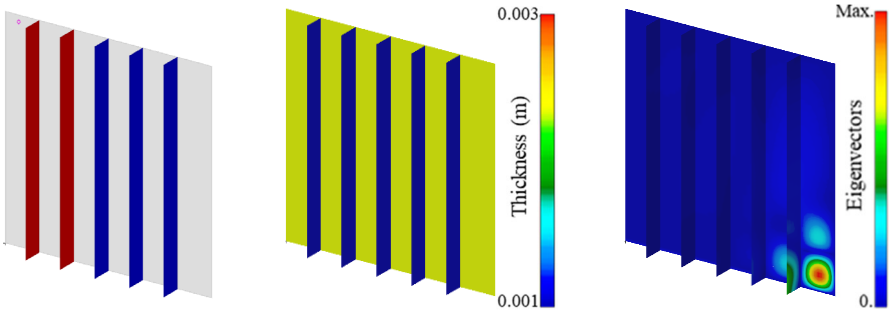

CAD Model, m = 0.660 kg Skin = 0.002325 m Mode 1 = 1.0

(b)

Skin Stiffener Ghost Stiffener

Fig. 14: Optimal design of a stiffened panel with 5 stiffeners: (a) Size optimal results; (b) Simultaneous size and topology optimal results

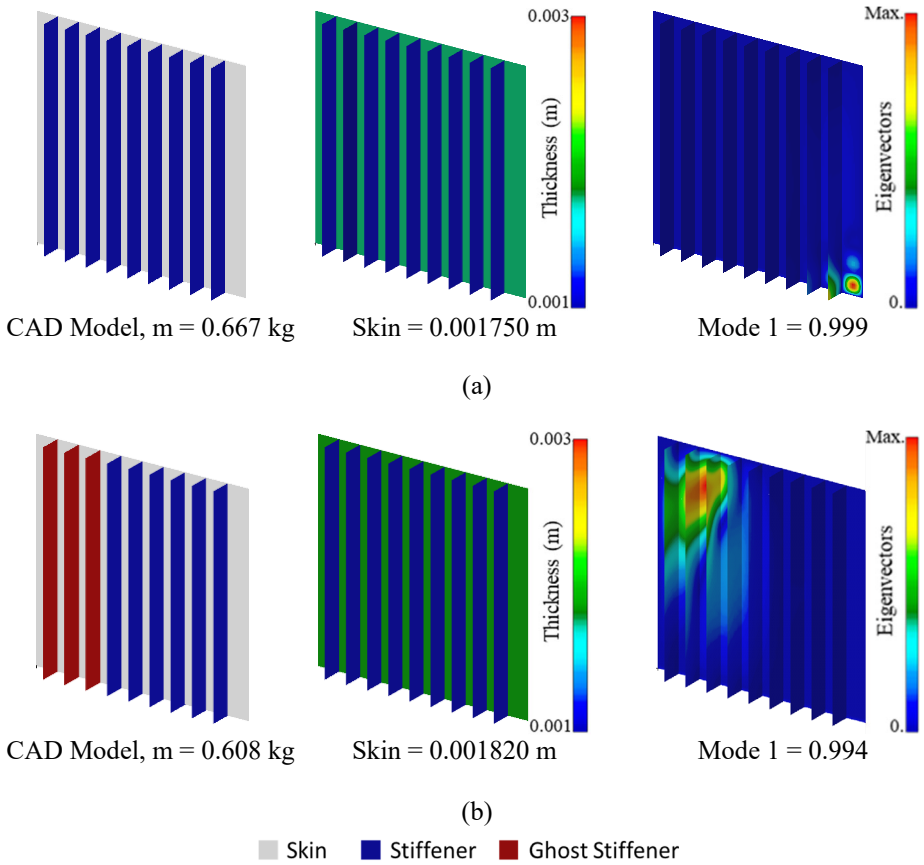

Fig. 15: Optimal design of a stiffened panel with 9 stiffeners: (a) Size optimal results; (b) Simultaneous size and topology optimal results

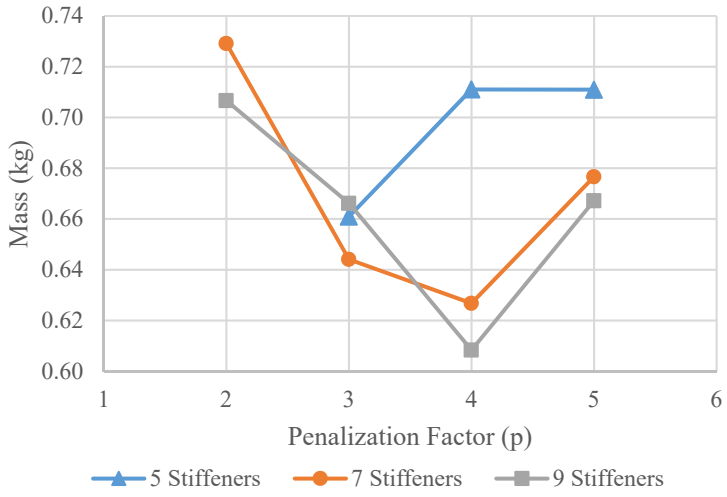

Fig. 16: Effect of initial designs with different numbers of stiffeners on the optimal mass

B. Simultaneous Size and Layout Optimization of the Stiffened Panel

The results of the optimal design achieved through the simultaneous size and layout optimization of a stiffened panel with 7 stiffeners are presented in Fig. 17. It can be seen that the stiffness of the panel is tailored predominantly by the movement of stiffeners towards the right side of the skin at the bottom edge. The trend herein observed is that the thicknesses of the skin and the stiffeners are reduced to their lower bounds and the stiffeners are shifted towards

the right end to meet the buckling constraints. It is evident from the eigenvectors that the skin underwent buckling at the top left corner of the panel in mode 1 and the global buckling modes were localized between the stiffeners. It is also observed that at the bottom edge of the skin, the first stiffener from the left side of the panel reached the maximum move limit allowed by the CAD-based parameterization herein employed. Therefore a further reduction in mass is expected by increasing the upper bound values of the layout variables. The benchmarking of these results against Ref. 8 is presented in the author's previous paper [20]. It can be concluded from the results presented here that the buckling response of the stiffened panel is more sensitive to its layout design variables than the size design variables when optimized simultaneously.

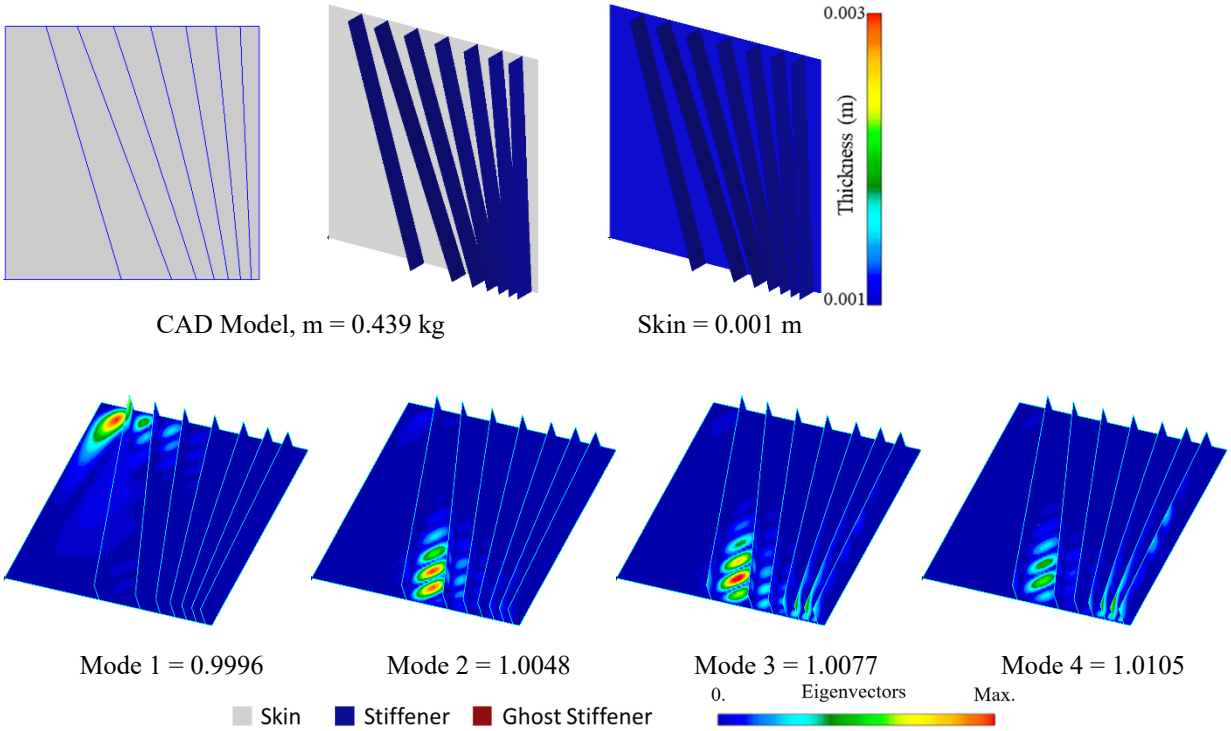

Fig. 17: Optimal design of the stiffened panel achieved through simultaneous size and layout optimization

C. Simultaneous Size, Layout, and Topology Optimization of the Stiffened Panel

Simultaneous size, layout, and topology optimization was conducted using different values of parameter p. The results of the optimal design achieved while using $p = 3.0$ are shown in Fig. 18. It can be observed that the thicknesses of the skin and stiffeners were reduced to their lower bounds. The stiffeners at the bottom edge of the skin were shifted towards the right end to meet the buckling constraint. The first stiffener from the left side of the panel became a ghost stiffener and this generated a loss of stiffness which was compensated purely through the change of layout. While comparing these results with the same achieved through the simultaneous size and layout optimization, it is observed that at the top edge of the skin, the stiffeners moved toward the left side of the panel to compensate for the loss of stiffness generated by the ghost stiffener. It is evident from the mode 1 eigenvector that the skin underwent buckling at the top left corner of the panel. The global buckling mode crossed the first stiffener because it was a ghost stiffener.

The results summary is tabulated in Table 3. In the optimal design achieved through simultaneous size, layout, and topology optimization while using $p = 4.0$, there was no ghost stiffener. The optimal mass, in this case, is similar to the same achieved through simultaneous size and layout optimization. The layout of both optimal designs is the same. The optimal mass achieved while using $p = 2.5$ is even higher than the same found through size optimization because in this case 4 stiffeners from the left side of the panel were transformed into ghost stiffeners. The loss of stiffness was compensated by an increase in the thickness of the skin. Thus, an inferior optimal design was found. From the results summary it can be concluded that the lowest optimal mass is achieved through the simultaneous size, layout, and topology optimization while using $p = 3.0$. In comparison to the initial design, a mass reduction of about 51% is achieved. This reinforces the previous conclusion that the lowest optimal mass can be ensured while using parameter

p in the range from 3.0 – 4.0. The next best optimal design is achieved through simultaneous size and layout optimization. Here a mass reduction of about 49% is attained. Although the lowest optimal mass is yielded by the former optimization, a slightly higher optimal mass at a relatively lower computational cost is found by the latter optimization.

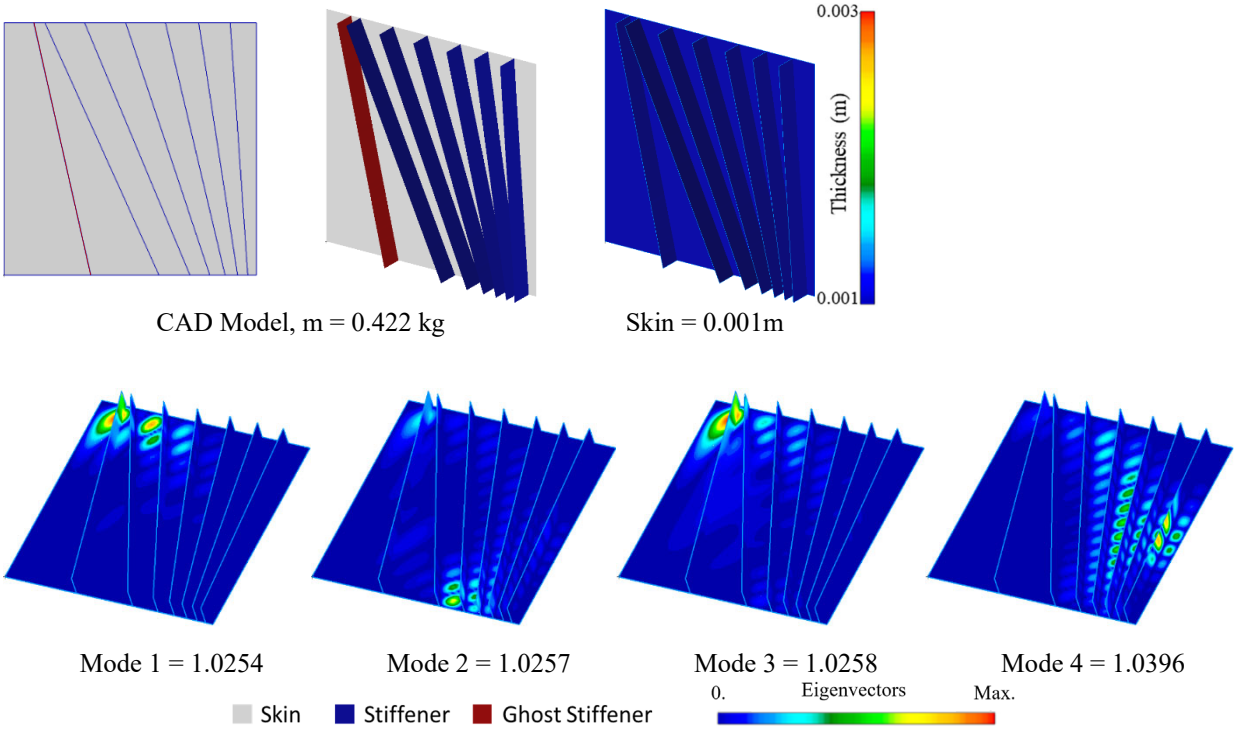

Fig. 18: Optimal design of the stiffened panel achieved through simultaneous size, layout, and topology optimization

Table 3: Results Summary

	Initial Design	**Size**	**Size + Topology ($p = 4$)**	**Size + layout**	**Size + Layout + Topology**		
					$p = 2.5$	$p = 3.0$	$p = 4.0$
BLF	1.106	0.9999	1.0010	0.9996	0.9997	0.9939	0.9999
Mass (Kg)	0.855	0.675	0.627	0.439	0.722	0.422	0.436
Mass Relative Difference (%)	-	21.05	26.67	48.65	15.56	50.64	49.01

VI. Conclusion

The proposed methodology successfully performs simultaneous size, layout, and topology optimization. This provides additional capability to locally tailor the structure. The buckling response of the stiffened panel is found more sensitive to the layout design variables than the size and topology design variables when optimized simultaneously. The use of re-meshing allows greater changes in the layout without mesh distortion. The CAD-based parameterization eliminates the requirement of additional constraints on grid point coordinates and allows the direct use of CAD models which is crucial for the wider adoption of this method in the industry. The number of stiffeners can only be a discrete value and is successfully optimized using a gradient-based optimizer. The use of analytical response sensitivities and the gradient-based optimizer makes the methodology especially suitable for preliminary design. The novel designs achieved through optimization can be easily manufactured without additional cost penalties. The proposed methodology is not limited to the stiffened panels only and can be used for the design of complex configurations such as a wing box or other thin-walled structures.

Acknowledgments

The authors would like to thank Ole Sigmund (DTU) and Christian Aparicio (the-engineering-lab) for sharing their experience and valuable inputs on the design methodology proposed in this paper. The authors are grateful to John Dannenhoffer (Syracuse University), Bob Haimes (MIT), and Ryan Durscher (AFRL) for their feedback on the proposed methodology and detailed technical discussions on ESP, NastranAIM, and sensitivities calculation. The authors would also like to thank Justin Gray (NASA) for his guidance related to OpenMDAO and CAD-based parameterization. The authors are also grateful to Sheng Chu (Cardiff University) for sharing his experience and the data related to the stiffened panel used in this paper.

References

[1] N. Aage, E. Andreassen, B. S. Lazarov, and O. Sigmund, "Giga-voxel computational morphogenesis for structural design," *Nature*, vol. 550, no. 7674, pp. 84–86, 2017, DOI: 10.1038/nature23911.

[2] Z. Wang, A. S. J. Suiker, H. Hofmeyer, T. van Hooff, and B. Blocken, "Coupled aero structural shape and topology optimization of horizontal-axis wind turbine rotor blades," *Energy Convers. Manag.*, vol. 212, no. February, p. 112621, 2020, DOI: 10.1016/j.enconman.2020.112621.

[3] S. Arranz, A. Sohouli, and A. Suleman, "Buckling optimization of variable stiffness composite panels for curvilinear fibers and grid stiffeners," *Journal of Composites Science*, vol. 5, no. 12. 2021, doi: 10.3390/jcs5120324.

[4] R. K. Kapania, J. Li, and H. Kapoor, "Optimal design of unitized panels with curvilinear stiffeners," *Collect. Tech. Pap. - AIAA 5th ATIO AIAA 16th Light. Syst. Technol. Conf. Balloon Syst. Conf.*, vol. 3, no. September, pp. 1708–1737, 2005, DOI: 10.2514/6.2005-7482.

[5] M. Bhatia, R. K. Kapania, and D. Evans, "Comparative study on optimal stiffener placement for curvilinearly stiffened panels," *J. Aircr.*, vol. 48, no. 1, pp. 77–91, 2011, DOI: 10.2514/1.C000234.

[6] B. Colson, M. Bruyneel, S. Grihon, C. Raick, and A. Remouchamps, "Optimization methods for advanced design of aircraft panels: A comparison," *Optim. Eng.*, vol. 11, no. 4, pp. 583–596, 2010, DOI: 10.1007/s11081-008-9077-8.

[7] S. B. Mulani, W. C. H. Slemp, and R. K. Kapania, "EBF3PanelOpt: An optimization framework for curvilinear blade-stiffened panels," *Thin-Walled Struct.*, vol. 63, pp. 13–26, 2013, DOI: 10.1016/j.tws.2012.09.008.

[8] S. Chu, S. Townsend, C. Featherston, and H. A. Kim, "Simultaneous size, layout and topology optimization of stiffened panels under buckling constraints," *AIAA SciTech 2021 Forum*, no. January, pp. 1–19, 2021, DOI: 10.2514/6.2021-1894.

[9] S. Chu, S. Townsend, C. Featherston, and H. A. Kim, "Simultaneous layout and topology optimization of curved stiffened panels," *AIAA J.*, vol. 59, no. 7, pp. 2768–2783, 2021, DOI: 10.2514/1.J060015.

[10] S. Chu, C. Featherston, and H. A. Kim, "Design of stiffened panels for stress and buckling via topology optimization," *Struct. Multidiscip. Optim.*, vol. 64, no. 5, pp. 3123–3146, 2021, DOI: 10.1007/s00158-021-03062-3.

[11] R. Haimes and J. F. Dannenhoffer, "The engineering sketch pad: A solid-modeling, feature-based, web-enabled system for building parametric geometry," *21st AIAA Comput. Fluid Dyn. Conf.*, pp. 1–21, 2013, DOI: 10.2514/6.2013-3073.

[12] J. Joe, V. Gandhi, J. F. Dannenhoffer, and H. Dalir, "Rapid generation of parametric aircraft structural models," *AIAA SciTech 2019 Forum*, no. January, pp. 1–10, 2019, DOI: 10.2514/6.2019-2229.

[13] J. F. Dannenhoffer and R. Haimes, "Design sensitivity calculations directly on CAD-based geometry," *53rd AIAA Aerosp. Sci. Meet.*, pp. 1–25, 2015, DOI: 10.2514/6.2015-1370.

[14] R. A. Canfield, S. Alnaqbi, R. J. Durscher, D. E. Bryson, and R. M. Kolonay, "Shape continuum sensitivity analysis using Astros and caps," *AIAA SciTech 2019 Forum*, 2019, DOI: 10.2514/6.2019-2228.

[15] MSC.Software, "Design Sensitivity and Optimization User's Guide," *MSC.Software Corp.*, 2005, [Online]. Available: http://www.kxcad.net/MSC_Software/nastran/prior_release/2005_nastran_release_guide.pdf.

[16] M. P. Bendsøe and O. Sigmund, *Topology Optimization, Theory, Methods, and Applications*. 2004.

[17] B. K. Stanford, "Optimal control surface layout for an aeroservoelastic wingbox," *AIAA J.*, vol. 55, no. 12, pp. 4347–4356, 2017, DOI: 10.2514/1.J056070.

[18] J. S. Gray, J. T. Hwang, J. R. R. A. Martins, K. T. Moore, and B. A. Naylor, "OpenMDAO: an open-source framework for multidisciplinary design, analysis, and optimization," *Struct. Multidiscip. Optim.*, vol. 59, no. 4, pp. 1075–1104, 2019, DOI: 10.1007/s00158-019-02211-z.

[19] R. Durscher and D. Reedy, "Pycaps: A python interface to the computational aircraft prototype syntheses," *AIAA SciTech 2019 Forum*, no. January 2019, DOI: 10.2514/6.2019-2226.

[20] H. Rahman, R. De Breuker, and S. G. P. Castro, "Optimal Design of Stiffened Panels Under Buckling Loads : a Design Methodology Considering Cad-Based Parameterization With Simultaneous Layout and Sizing," in *33rd Congress of the International Council of the Aeronautical Sciences*, 2022, September, [Online]. Available: https://www.icas.org/ICAS_ARCHIVE/ICAS2022/data/preview/ICAS2022_0393.